

# Measuring co-seismic deformation of the Fandoqa (14/03/98 - Mw 6.6) and Zirkuh (10/05/97 - Mw 7.1) earthquakes, SE Iran.

*Peyret, M., Cadoul, B., Chéry, J.*

*Laboratoire de Dynamique de la Lithosphère, Université de Montpellier II, France*

## 1. Introduction

The Arabia-Eurasia convergence (~25 mm/year, figure 1) is accommodated in Iran in the Zagros (SW), the Kopeh Dag (NE) and the Alborz (N) belts. The shortening that is not taken up in the Zagros mountains leads to N-S right lateral shear on both sides of the aseismic rigid block of the Dasht-e-Lut (figure 2)..

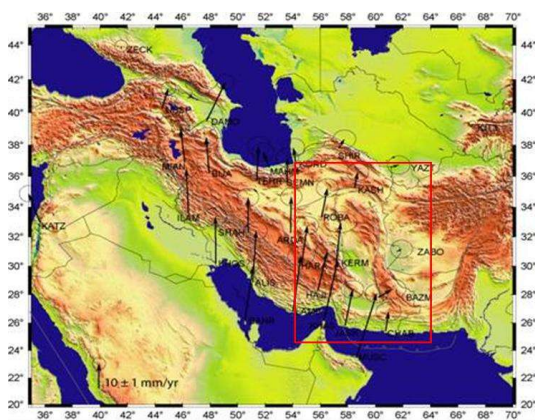


Figure 1: GPS velocity field with respect to fixed Eurasia, P. Vernant et al. 2003

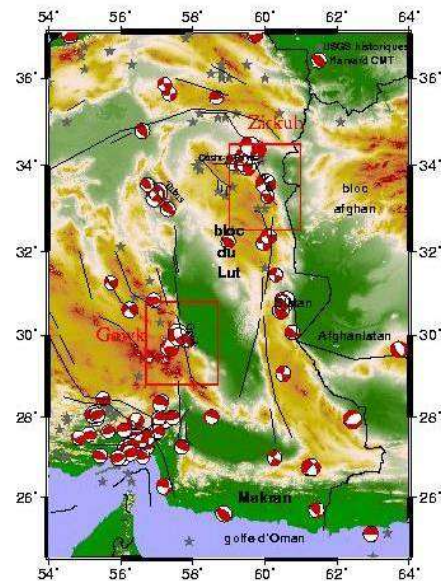


Figure 2: Right lateral shear systems of Eastern Iran

The complex fault systems of Gowk (West) and Zirkuh (East) re-ruptured in the last decades. They are examples of clusters of earthquakes, which makes their analysis interesting from a stress change point of view. The InSAR technique applied to archives spanning 4 years before the earthquakes does not reveal any significant fringe patterns that could be interpreted as deformation expressing some stress change induced by past earthquakes. The time interval between the past events (1979 or 1981) and the ERS mission, associated with the relative small coseismic surface deformation may explain this lack of signal. So we focus on Fandoqa (14/03/98 - Mw 6.6) and Zirkuh (10/05/97 - Mw 7.1) co-seismic displacements.

## 2. InSAR

The archived ERS data are not numerous on these two zones. But, it was possible to map this coseismic deformation by InSAR (figure 3, 5) and to compute the synthetic interferograms for both earthquakes (figure 4, 6) by forward transformation. We use information relative to the slip at depth and the fault geometry provided in the literature by Berberian et al.

In the case of the Fandoqa earthquake, the interferogram reveals some slip on the Shahdad thrust fault (mapped in yellow in figure 4) that may have been triggered by the Fandoqa earthquake. The model at depth uses the following characteristics. For the Gowk fault: dip=56°W, depth=7km, strike-slip=1.1m, dip-slip=0.75m. For the Shahdad thrust fault: dip=10°W, depth=1-4km, thrust-slip=0.07m.

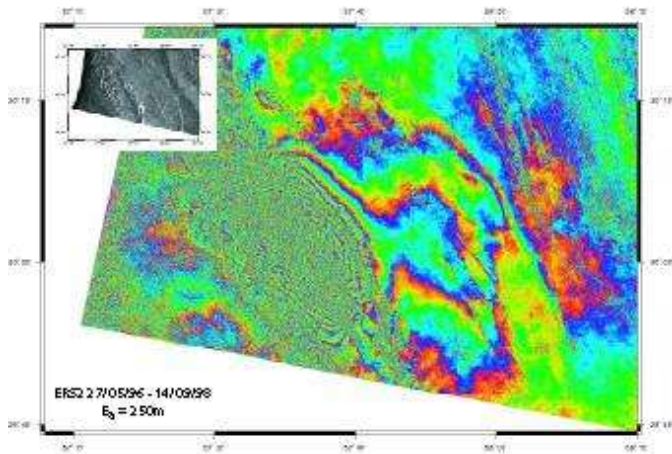


Figure 3: Coseismic differential interferogram of the Fandoqa earthquake

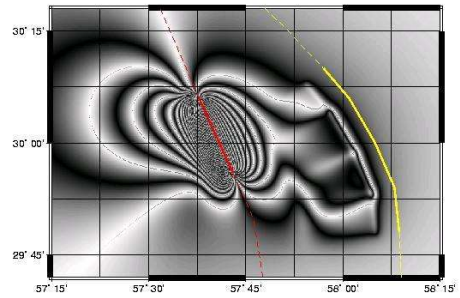


Figure 4: Synthetic interferogram using information at depth provided by Berberian et al. 2000.

The Abiz Fault ruptured on 120km due to the Zirkuh earthquake. The coseismic deformation fringes cover more than 2 scenes, but they appear quite clearly on the southern track, while, to the north, heavy temporal decorrelation is observed. So we propose a model at depth for the southern extremity of the rupture. We use 3 consecutive segments which parameters, from North to South, are: // dip  $85^{\circ}$ W, depth=15km, strike-slip=2.5m,dip-slip=0m // dip  $65^{\circ}$ W, depth=15km, strike-slip=3.5m,dip-slip=0.1m // dip  $65^{\circ}$ W, depth=6km, strike-slip=1m,dip-slip=0.45m . This model is in good agreement with the observed fringes. Nevertheless, it is difficult to fit the model to the small spatial extend details of the southern end of the rupture. May be, because after slip occurred in addition to coseismic deformation.

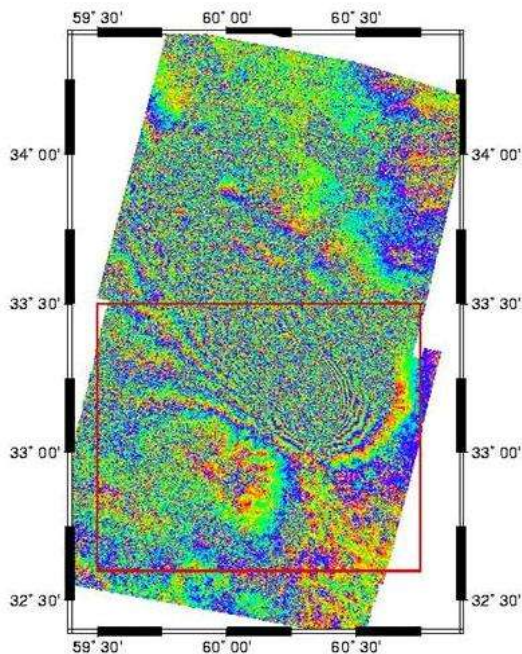


Figure 5: Mosaic of coseismic interferograms of the Zirkuh earthquake

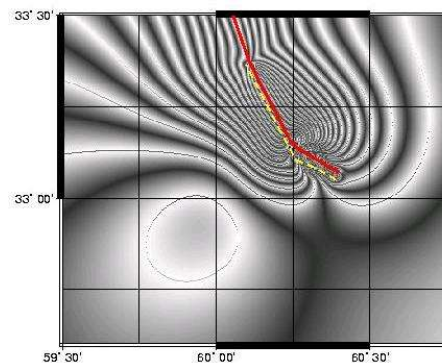


Figure 6: Synthetic interferogram of the southern part of the rupture using multiple segments at depth

### 3.Offsets determined by sub-pixel correlation

In the case of these earthquakes that took place in a transpressive context, using only descending orbits makes impossible to discriminate right lateral strike slip component from any other normal component. In order to complement InSAR data, we map accurately the surface rupture and get an estimation of the horizontal surface displacement by using sub-pixel correlation methods applied on both Spot (figure 7, 8) and ERS SAR amplitude images (figure 9). The resolution of the Spot panchromatic images is 10m and the discontinuity across the fault is about 0.1 pixel both in line and column direction. The horizontal component is then estimated to 1.5m along most parts of the rupture. A similar estimation can be done in the azimuth and distance directions with SAR amplitude images.

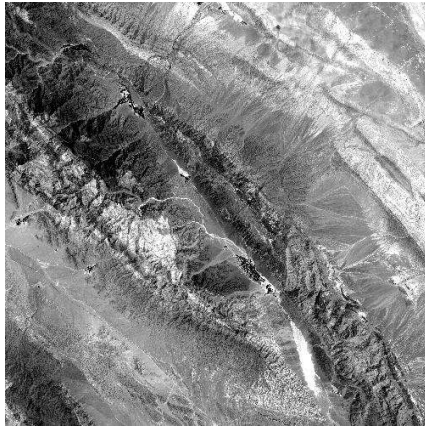


Figure 7: Spot image (10m resolution) of the Fandoqa fault zone

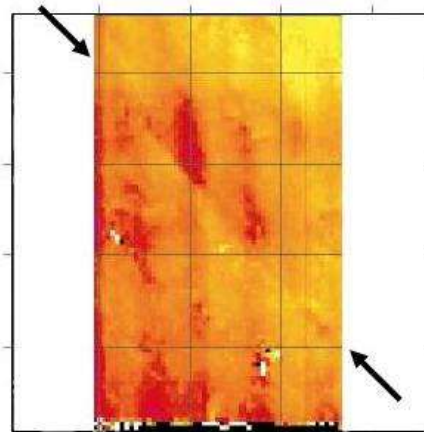


Figure 8: discontinuity of the offsets across the fault revealed by sub-pixel correlation on Spot images.

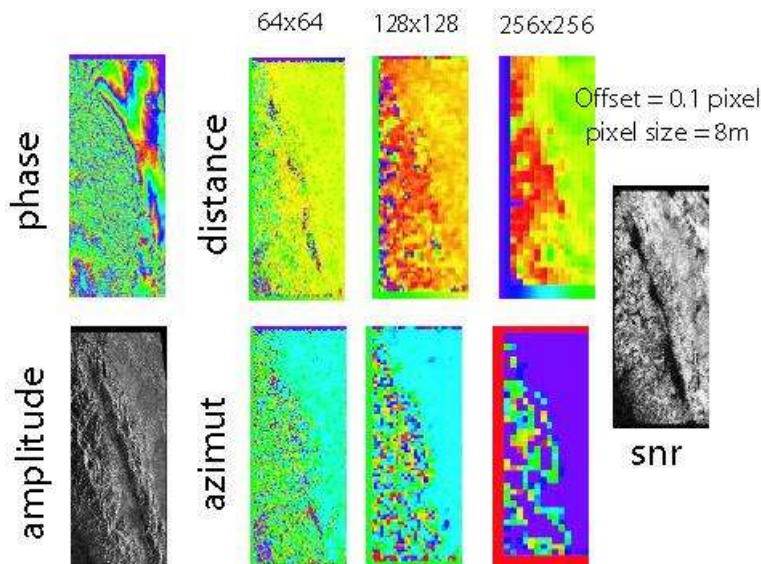


Figure 9: discontinuity of the offsets across the fault revealed by sub-pixel correlation on SAR amplitude channels.

### 4. Inversion procedure

Finally, we propose an inversion method (figure 10) that can invert jointly surface measurements obtained by InSAR or GPS, in order to infer models for coseismic slip distribution at depth. Displacements are calculated using an elastic dislocation buried within a homogeneous elastic half-space. We impose the fault geometry and derive the slip distribution in depth using a

generalised least square method with smoothing. It consists in minimising the roughness of the model, together with its distance to an a-priori model, under the constraint that the predicted surface deformations do not differ significantly from the observed ones. We illustrate the use of this technique for the Fandoqa earthquake (figure 11). We digitalise fringe limits and invert this deformation data projected along the satellite line of sight. The fault geometry has been imposed and the ruptured fault segment has been divided in 1 or 9 patches. The slip vector at depth is computed for each patch. The predicted surface displacement is in good agreement with the observed fringes.

**Inversion procedure** (adapted from A. Loevenbrück)

slip model constrained by the data  $\mathbf{Wd} = \mathbf{WPGm}$

roughness of the model  $R = \|\delta m\|^2$

a priori model  $\mathbf{H} = \mathbf{Fm}$

$\mathbf{m}$  slip distribution model at depth  
 $\mathbf{d}$  InSAR measurements  
 $\mathbf{W}$  Weighting function  
 $\mathbf{P}$  Projection along the line of sight  
 $\mathbf{G}$  Okada forward transform  
 $\delta$  First derivative  
 $\mu$  Lagrange multipliers

**Pb:** unconstrained functional  $\mu^{-1} \|\mathbf{H} - \mathbf{Fm}\|^2 + \mu_0^{-1} \|\delta m\|^2 + \|\mathbf{Wd} - \mathbf{WPGm}\|^2$

$\mu$  is selected iteratively until the difference between the estimated moment and the seismic moment is small

Figure 10: Principle of the inversion procedure

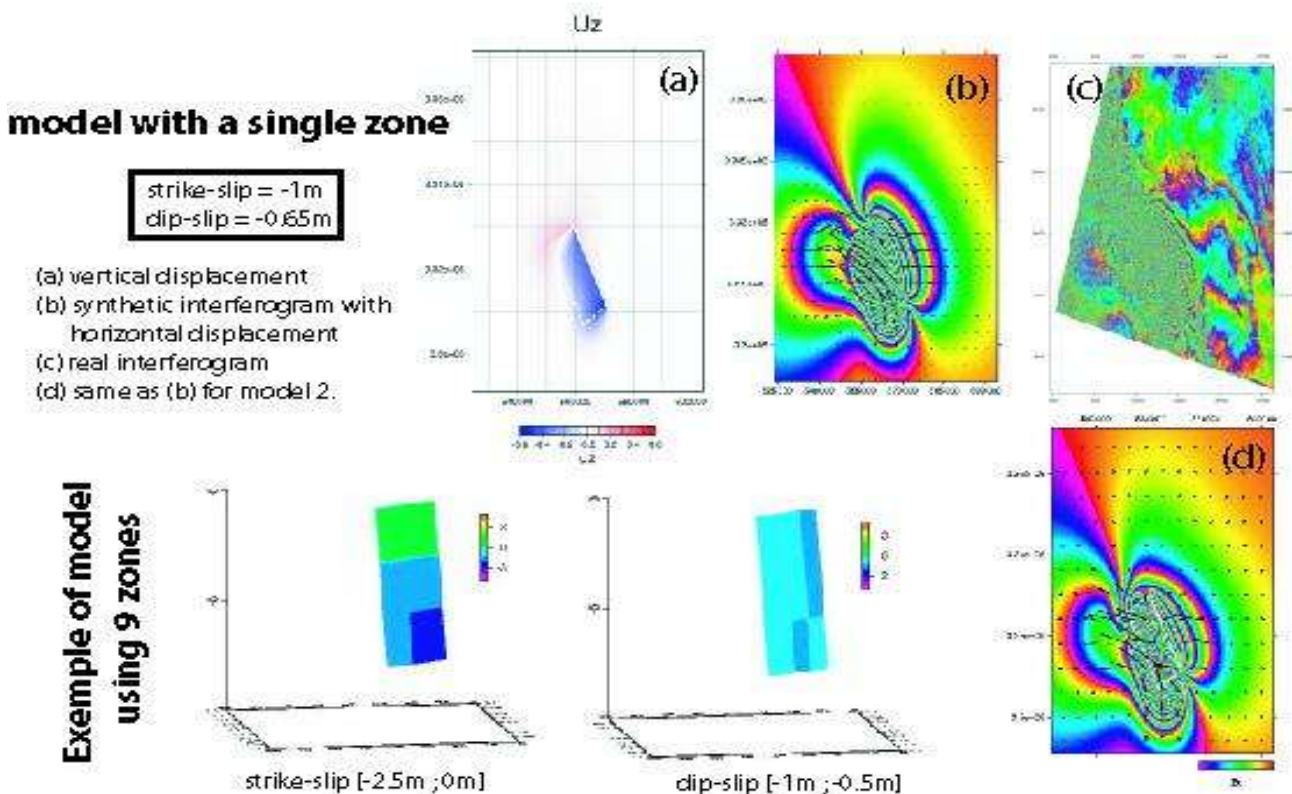


Figure 11: Illustration of the inversion procedure for the Fandoqa earthquake

## **Conclusion**

In the framework of the InSAR analysis of the co-seismic displacement field generated by the Fandoqa and Zirkuh earthquakes, we have illustrated the use of complementary techniques like sub-pixel correlation. Although the spatial resolution and the deformation estimation are lower, this technique provides a precise location of the surface rupture and gives insights on the 3D surface deformation. Finally we proposed an inversion method that can invert jointly GPS and InSAR measurements.